Design of a High-Precision Hemodynamic Module Based on the AD7124

Xingze Wang, and Feng Wang*

School of Biological Science & Medical Engineering, Southeast University, Nanjing, China

Abstract. This study presents the design and implementation of a high-precision, multi-channel hemodynamic acquisition module for synchronous invasive blood pressure monitoring. The system adopts a modular hardware architecture integrating differential signal conditioning, low-noise amplification, multi-level protection, a 24-bit Σ–Δ ADC (AD7124), and an STM32F205-based controller for data management and communication. Quasi-synchronous sampling of three pressure channels is achieved with independently configurable sampling rates and gains, while firmware based on STM32CubeHAL ensures accurate timing control and data framing. Experimental results from mock-loop testing demonstrate high static accuracy, reliable linearity, and preliminary bench-top verification of dynamic waveform acquisition capability and inter-channel skew within 10 μs. The proposed module features compact size, low power consumption, and scalable channel capability, and can be readily integrated into existing monitoring systems or experimental platforms, providing a stable and high-fidelity data acquisition front end for hemodynamic research and algorithm development.

1 Introduction

Clinical hemodynamic monitoring plays a central role in perioperative management, intensive care, and cardiovascular assessment by providing continuous and reliable information on circulatory status, including arterial blood pressure, central venous pressure, and pulmonary artery pressure[1, 2]. Among existing techniques, the pulmonary artery catheter remains an important reference method because it can directly measure right-heart and pulmonary circulation pressures and supports cardiac output estimation through thermodilution. However, its operation is invasive and technically demanding, and its clinical use is limited by risks such as arrhythmia, thrombosis, infection, and vascular injury. In comparison, invasive blood pressure monitoring based on pressure transducers is more widely adopted in clinical practice because it enables continuous waveform acquisition with higher temporal resolution and stronger resistance to motion artefacts than non-invasive cuff-based methods[3]. In addition to providing instantaneous pressure values, high-quality invasive pressure waveforms also support the extraction of dynamic hemodynamic indices such as pulse pressure variation and stroke volume variation, which are valuable for fluid management and therapeutic evaluation.

With the increasing demand for refined monitoring and intelligent analysis, conventional monitoring devices still face several limitations in research and practical applications[4, 5]. Commercial systems often provide restricted access to raw waveform data, insufficient acquisition precision, limited channel scalability, or relatively large inter-channel delay, which makes them less suitable for algorithm development, multi-parameter synchronous analysis, and preclinical experimental studies. Existing studies have shown the importance of low-noise front-end design, high-resolution analog-to-digital conversion, and electrical safety isolation in invasive physiological signal acquisition, but there remains a need for a compact and extensible module capable of high-precision, multi-channel, and quasi-synchronous acquisition[6, 7].

To address these issues, this study designs a high-precision multi-channel hemodynamic acquisition module based on the AD7124 and STM32F205[8]. The proposed system integrates differential signal conditioning, low-noise amplification, filtering, multi-level protection, 24-bit analog-to-digital conversion, embedded timing control, and serial communication into a modular architecture. It supports quasi-synchronous acquisition of three invasive pressure channels with independently configurable gain and sampling rate, while maintaining low noise and microsecond-level inter-channel synchronization. The aim is to provide a stable, reliable, and scalable front-end platform for invasive hemodynamic waveform acquisition, thereby supporting subsequent signal processing, parameter extraction, and intelligent monitoring research.

The main innovations of this work are as follows:

1. A miniaturized design based on the open-source STM32CubeHAL driver framework compresses the traditional front-end circuits of bedside monitors,

* Corresponding author: 220214945@seu.edu.cn

enabling direct deployment near the operating table or integration into existing monitoring systems.

2. Raw 24-bit data are transmitted without compression via RS232, providing a high-resolution, uncompressed, and time-aligned waveform interface for research and algorithm development. This addresses existing limitations of commercial devices, whose raw data interfaces are often closed, have insufficient bit depth (≤16 bit), or exhibit excessive inter-channel delay (>200 ms). In contrast, the typical latency of the proposed module is 8–9 ms.

3. The bill-of-materials cost per module is relatively low, achieving a balance among accuracy, cost, and multi-channel synchronization.

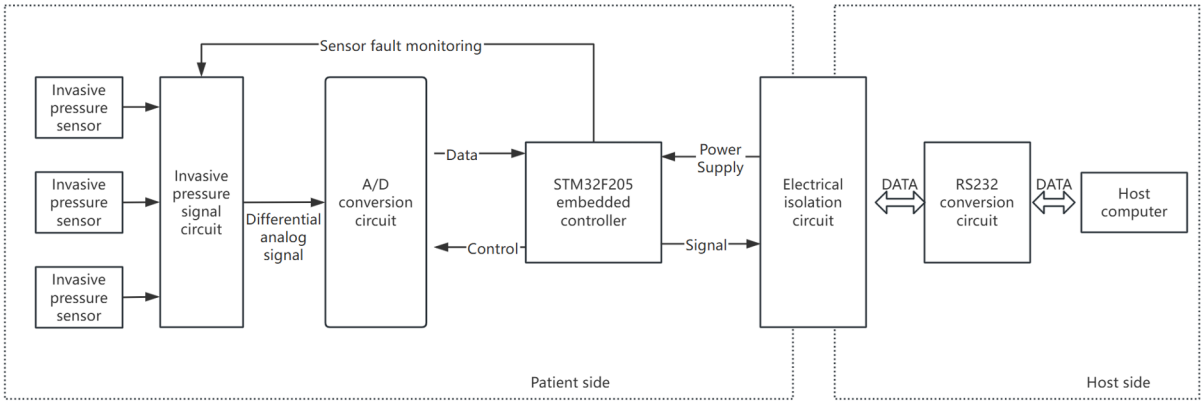

Figure 1. Overall block diagram of the hemodynamic monitoring module

The module can serve as a standardized "plug-and-play" data front end for preclinical research, AI algorithm training, and secondary development of high-end monitors[9], thereby addressing current gaps in data accessibility and signal quality in commercially available systems.

2 Hardware design framework of the hemodynamic monitoring module

To satisfy the requirements of invasive hemodynamic monitoring for high accuracy, low noise, real-time response, and multi-channel scalability, a modular acquisition architecture was developed based on a complete signal chain extending from the pressure transducer to the host computer. As illustrated in Figure 1, the proposed system consists of an analog front end, a high-resolution analog-to-digital conversion stage, a digital control and communication unit, and an electrically isolated power and interface subsystem. This architecture was designed to preserve weak physiological signals with high fidelity while ensuring patient safety and reliable operation in clinical or experimental environments.

At the input stage, invasive blood pressure signals generated by disposable pressure transducers are first routed to a dedicated analog front end. Because these signals are millivolt-level differential outputs that are highly susceptible to electromagnetic interference, baseline drift, and electrostatic discharge, the front end integrates differential signal conditioning, low-noise amplification, analog filtering, and multi-level protection. A symmetrical amplification topology based on a precision low-noise operational amplifier is adopted to improve the signal-to-noise ratio while suppressing common-mode interference. In parallel, current-limiting resistors and clamping devices are introduced at the input to provide protection against electrostatic discharge and transient overvoltage without significantly degrading input impedance or waveform integrity. The analog filtering network is configured to preserve the principal spectral content of invasive pressure waveforms while attenuating high-frequency environmental and electrosurgical interference, thereby enabling stable and faithful waveform reconstruction.

The conditioned analog signal is digitized by the AD7124, a 24-bit Σ–Δ ADC that integrates a programmable gain amplifier and flexible digital filtering functions. This device was selected to meet the dual requirement of high resolution and low input-referred noise in physiological signal acquisition. In the present design, the converter operates in single-conversion mode and sequentially samples three invasive pressure channels under timer-based control. To accommodate the different temporal characteristics of monitored signals, the primary waveform channel is sampled at 500 Hz, whereas the remaining channels are sampled at 125 Hz. Although the AD7124 employs a single conversion core, quasi-synchronous acquisition is achieved through deterministic scheduling by the microcontroller and rapid SPI readout, allowing the system to maintain microsecond-level inter-channel timing consistency. Different digital filter settings are further assigned according to channel function so that the high-speed channel favors low latency, whereas the slower channels prioritize improved noise suppression.

System control and data management are performed by an STM32F205 microcontroller, which coordinates ADC triggering, SPI communication, data buffering, frame packaging, and host-side transmission. Benefiting from hardware support for DMA, CRC, and multiple interrupt sources, the controller can sustain real-time acquisition while minimizing processor overhead and the risk of data loss. The embedded firmware was developed on the STM32CubeHAL framework and implements peripheral initialization, timer-driven sampling, communication parsing, and basic fault monitoring. To

ensure robust data transfer, the output protocol incorporates frame headers, length information, sequence indexing, and checksum verification, enabling reliable reception and reconstruction of raw waveform data at the host computer.

Because the system is intended for use in medical monitoring scenarios, electrical isolation and interface robustness were treated as integral parts of the hardware design rather than auxiliary features. A medical-grade isolated power supply and digital isolation devices are used to separate the patient-side analog circuitry from the host-side digital and communication circuits, thereby reducing common-mode coupling and preventing unsafe leakage currents. The internal UART communication is subsequently converted to RS-232 levels for external interfacing, which improves compatibility with existing monitoring platforms and laboratory acquisition systems. Additional decoupling, filtering, and level-shifting circuitry are introduced around the converter, isolators, and communication driver to stabilize the supply rails and suppress switching noise, thus preserving the effective resolution of the ADC.

Table 1. Functional summary of signal-conditioning stages in the signal chain

Unit	Function	Key specifications / safety points
IBP sensor	Converts pressure to mV-level differential signal	Sensitivity: 5 μV/V/mmHg at 5 V; isolated excitation; anti-backflow design
Protection circuit	ESD, surge, and overvoltage protection	TVS + RC limiting; ±8 kV contact discharge; IEC 60601-1-2 compliant
Instrumentation amplifier	Amplifies weak differential signal for ADC input	Gain: 50–200×; offset/drift compensation; CMRR ≥ 100 dB
Filter stage	Suppresses noise while preserving pressure waveform	Passband: 0.5–40 Hz; preserves arterial-pressure bandwidth
AD7124 ADC	High-resolution digitization	24-bit Σ–Δ ADC; 125–500 sps; high input impedance
STM32F205 MCU	Sampling control, processing, and communication	Supports PPV/trend processing; watchdog; error detection
Isolation circuit	Electrical isolation between patient side and host	Isolation withstand voltage ≥ 4 kVrms; IEC 60601-1 compliant [10]
RS232 interface	Host communication	Baud rate up to 115200 bps; CRC/data validation supported

Overall, the proposed hardware framework achieves an effective balance among measurement precision, synchronization performance, electrical safety, and implementation complexity. Its modular structure facilitates direct integration into existing bedside monitors or animal experiment platforms and provides a stable front-end basis for subsequent hemodynamic analysis, parameter extraction, and algorithm development. The functional roles and key technical characteristics of the major stages in the signal chain are summarized in Table 1.

3 Software control logic design of the hemodynamic monitoring module

The software control logic of the proposed hemodynamic monitoring module was implemented as an embedded real-time framework responsible for acquisition scheduling, data handling, fault supervision, and host communication. Built on the STM32Cube development environment and the HAL driver library, the firmware was designed to coordinate the AD7124-based front-end acquisition hardware with the STM32F205 controller in a deterministic and low-latency manner. The software architecture emphasizes three key objectives: accurate multi-channel sampling, reliable data trans mission, and stable system operation under continuous monitoring conditions.

To ensure high-fidelity acquisition of invasive blood pressure signals, the AD7124 was configured with parameters optimized for low-frequency physiological waveform measurement. A Sinc3 digital filter was selected because it provides a favorable compromise between noise suppression, passband linearity, and settling time, making it suitable for dynamic pressure waveform acquisition. The internal post-filter and built-in 50/60 Hz rejection functions were disabled to avoid additional phase distortion and latency, while mains interference was instead controlled through analog filtering and overall electromagnetic compatibility design. The converter was referenced to an external precision voltage source to improve long-term stability and conversion consistency, and the programmable gain amplifier was set to 128× in order to maximize the effective utilization of the ADC input range for the low-level differential output of the pressure transducer. In addition, the burnout-current function was disabled to minimize sensor loading and reduce bias-related errors in the analog front end.

A central challenge in the software design was the realization of multi-rate acquisition using a single-conversion-core ADC. In the target configuration, one pressure channel was required to operate at 500 Hz for high-speed waveform capture, whereas the remaining two channels were sampled at 125 Hz for slower hemodynamic trends. Because the AD7124 performs channel conversion sequentially rather than truly simultaneously, the firmware adopted a timer-driven scheduling strategy to enforce deterministic sampling intervals. The TIM2 peripheral was configured to generate an interrupt every 2 ms, and this interrupt served as the fundamental sampling clock for channel sequencing. The primary channel was sampled during every cycle, whereas the remaining two channels were activated once every four cycles, thereby producing an effective sampling pattern of 500 Hz and 125 Hz, respectively. This time-division scheme enabled quasi-synchronous multi-channel operation while maintaining strict control over timing behavior. The overall logic of the sampling scheduler is illustrated in Figure 2.

To preserve real-time performance, the sampling interrupt was assigned the highest priority in the firmware. Within each interrupt cycle, the controller initiates ADC

conversion, waits for data-ready signaling, and reads the digitized result through SPI. The total time required for conversion and readout was verified experimentally by toggling a GPIO pin at the entry and exit of the interrupt service routine. Under the selected configuration, the total execution time was approximately 650 μs, which remained well below the 2 ms scheduling interval and therefore guaranteed that no cycle overrun occurred. This result confirms that the software timing design satisfies the real-time requirements of the acquisition task.

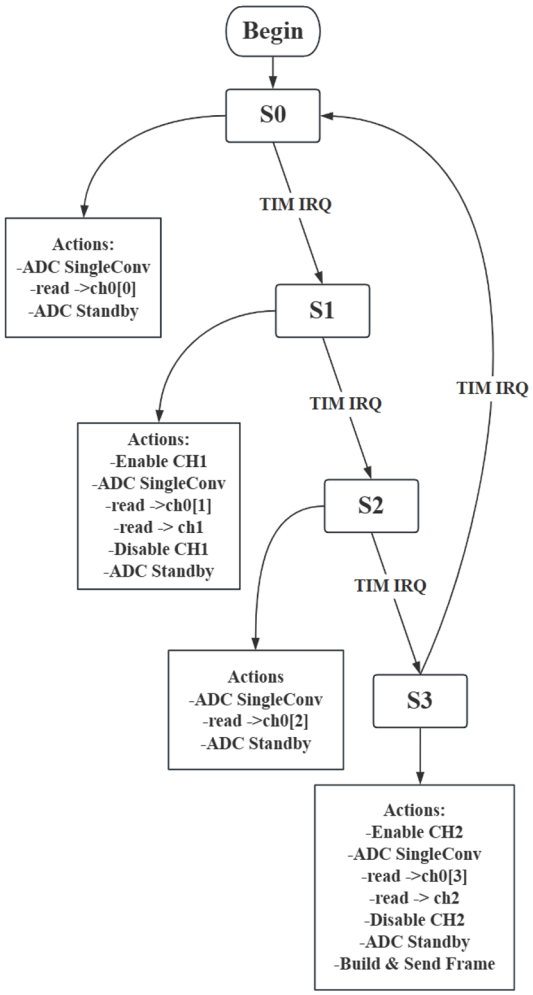

Figure 2. State machine for multi-channel sampling

In parallel with waveform acquisition, the firmware also performs periodic fault supervision for each sensor interface. The detection signals associated with disposable sensor connectivity are routed to the internal 12-bit ADC of the STM32F205 and sampled once per second. By comparing the measured voltage against predefined threshold ranges, the software classifies the channel state as normal, open-circuit, or short-circuit, and then packages the corresponding diagnostic information for transmission to the host. This mechanism improves operational robustness by enabling continuous online verification of sensor status without interfering with the main waveform acquisition process.

Communication between the module and the host computer was implemented using a UART-DMA framework combined with idle-line interrupt detection. In this scheme, incoming command frames are received automatically by DMA, and the USART IDLE interrupt is used to identify the end of each frame when no further data arrive within one character period. Only preliminary validation and length confirmation are executed in the interrupt context, whereas detailed parsing and command execution are deferred to the main loop. This design minimizes processor overhead and prevents lengthy communication tasks from disrupting high-priority sampling events. The UART interrupt was therefore assigned a lower priority than the timer-driven acquisition task, reflecting a sampling-first scheduling strategy.

To standardize host–device interaction, the module employs a lightweight serial communication protocol that supports configuration commands, acknowledgments, waveform transmission, and fault-status reporting. Each frame contains a fixed header, a payload-length field, a sequence index, the payload itself, a CRC byte, and a fixed frame tail. This structure facilitates synchronization, integrity verification, and packet tracking during continuous transmission. The format of the standard interaction frame is summarized in Table 2.

Table 2. Standard interaction frame format

Field	Description	Size
Frame header	Fixed header (0xAA 0xAA 0xAA)	3B
Data length	Length of the payload field	1B
Frame index	Sequential frame counter	2B
Data payload	data_length − 2 bytes	NB
CRC	Cyclic redundancy check	1B
Frame tail	Fixed tail (0xFF 0xFF 0xFF)	3B

Overall, the software control logic establishes a deterministic and scalable embedded framework for quasi-synchronous multi-channel hemodynamic acquisition. Through coordinated timer scheduling, optimized ADC control, asynchronous communication handling, and periodic fault supervision, the firmware provides a reliable basis for stable long-term monitoring and high-quality waveform data transmission.

4 Results

4.1 Hardware implementation

The fabricated prototype of the hemodynamic acquisition module is shown in Figure 3. The assembled printed circuit board integrates the analog front end, isolation circuitry, AD7124-based conversion stage, and STM32-based digital control unit within a compact modular layout. The prototype verified the feasibility of the proposed hardware architecture and provided the platform for subsequent experimental evaluation.

4.2 Bench-top performance evaluation

Bench-top experiments were performed using a pressure signal simulator that generated electrical outputs equivalent to those of a clinical pressure transducer. The simulator was connected directly to the sensor input of the module, and the acquired data were transmitted to the host

computer through the serial interface. The received packets were decoded in MATLAB to reconstruct the raw waveform for quantitative analysis.

Figure 3. Main board of the hemodynamic monitoring module

Static performance was first assessed under a constant-pressure condition corresponding to 150 mmHg. The recorded result is shown in Figure 4. Across 8,000 sampled points, the peak-to-peak variation of the ADC output was 3,532 counts. After compensation for the front-end gain of 128, the equivalent fluctuation referred to the transducer output was approximately 27.6 counts. The conversion factor between pressure and ADC counts was estimated from the transducer sensitivity and ADC resolution. The sensor sensitivity is

$$S = 5\mu V/V/mmHg \tag{1}$$

With a 5V excitation voltage(V_{ex}= 5V),the output voltage change for 1mmHg is:

$$\Delta V_{out} = S \times V_{ex} \times P \tag{2}$$

$$\Delta V_{out} = (5 \times 10^{-6}) \times 5 \times 1 = 25\mu V \tag{3}$$

For the 24-bit ADC with an input range of $-2.5$to $+2.5$ V, the voltage represented by one least significant bit is

$$1LSB = \frac{5}{2^{24}} \approx 0.298 \tag{4}$$

Therefore, the number of ADC counts corresponding to 1 mmHg is

$$Counts/\text{mmHg} = \frac{\Delta V_{out}}{1LSB} = \frac{25\mu V}{0.298\mu V} \approx 83.9 \tag{5}$$

According to the transducer sensitivity and ADC quantization relationship, a pressure change of 1 mmHg corresponds to approximately 84 ADC counts. The measured fluctuation therefore corresponded to an equivalent pressure variation of about 0.33 mmHg. This value is substantially below the commonly accepted 2 mmHg design target for invasive pressure monitoring, indicating good static stability and measurement precision.

Dynamic performance was preliminarily assessed using a 5 Hz sinusoidal electrical input. As shown in Figure 5, the reconstructed waveform followed the input trend and exhibited visually consistent periodicity in the time domain. In the frequency domain, the dominant spectral component was concentrated at the fundamental frequency, and no prominent spurious peaks were observed in the analyzed spectrum. These observations suggest that the proposed module can preserve the main low-frequency dynamic characteristics of the input signal under the present acquisition configuration. However, because this study did not include dedicated quantitative indices such as signal-to-noise ratio, harmonic distortion, or phase error, the dynamic evaluation should be regarded as a preliminary bench-top verification rather than a complete characterization of frequency-domain performance.

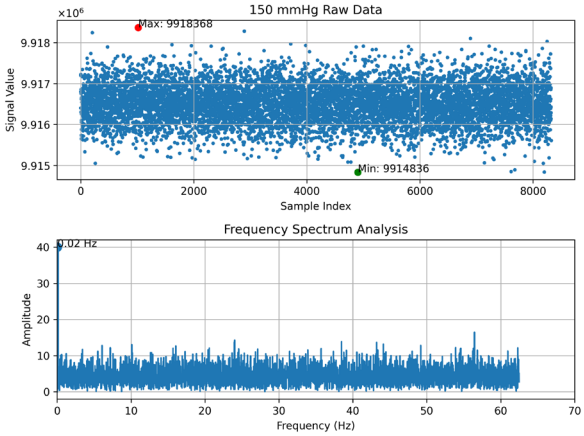

Figure 4. Test result for a 150 mmHg simulator output

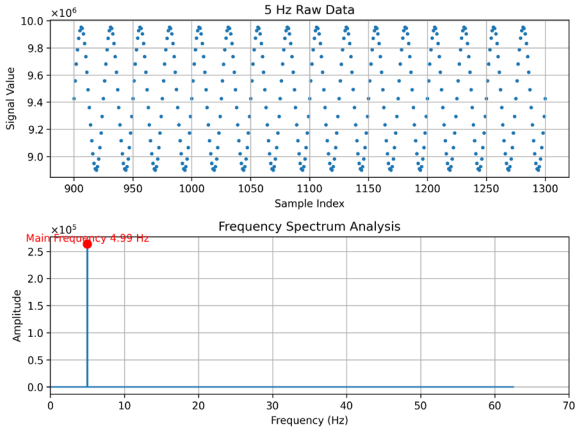

Figure 5. Time-domain waveform and corresponding spectrum of the acquired 5 Hz sinusoidal input signal used for preliminary dynamic performance assessment.

Overall, the bench-top tests verified high static precision and provided preliminary evidence of low-frequency dynamic waveform acquisition capability.

4.3 Fault-monitoring validation

The fault-monitoring function of the module was further evaluated using a dedicated fault-simulation fixture designed to emulate representative sensor-interface abnormalities. By applying different combinations of ten configurable switches, the fixture reproduced typical operating conditions, including normal connection, open-circuit faults, and short-circuit faults in the transducer

supply and signal lines. Under each test condition, the fault-monitoring module acquired the corresponding detection voltage through the internal ADC of the STM32, classified the sensor status according to the predefined decision thresholds, and reported the result to the host through the communication protocol.

The host computer decoded the received fault-status frames and compared the reported results with the known simulated conditions. The corresponding truth table of the fault-simulation fixture is summarized in Table 3. The measured ADC values under different fault conditions were clearly separated and were consistent with the threshold ranges defined in the fault-detection logic. In particular, disconnected probes and line faults produced distinct ADC responses, allowing reliable discrimination between normal and abnormal states. Experimental operation with different switch combinations confirmed that the proposed fault-monitoring module could correctly identify typical sensor faults and report them accurately in real time.

Table 3. Truth table of the sensor fault-monitoring simulation fixture

Test item	Fixture state SW1–SW10	Alarm message	Typical fault ADC value
Normal connection	00000 00000	No alarm	1570
Probe disconnected	11010 01000	Probe disconnected	250
IBP_5V line open	00000 01000	Probe disconnected	250
GND line open	00010 00000	Probe fault	2030
IBP+ line open	01000 00000	Probe fault	870
IBP− line open	10000 00000	Probe fault	870
IBP+ shorted to GND	00000 10000	Probe fault	420
IBP− shorted to GND	00001 00000	Probe fault	420
IBP+ shorted to +5 V	00000 00010	Probe fault	2030
IBP− shorted to +5 V	00000 00100	Probe fault	2030
IBP+ shorted to IBP–	00100 00000	No alarm	1570

4.4 Clinical waveform acquisition

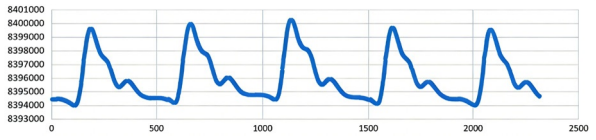

Figure 6. Clinical arterial blood pressure data from a patient

To examine the performance of the system under practical conditions, preliminary clinical waveform acquisition was carried out using arterial pressure data obtained from a patient in a hospital in Zhejiang Province. The recorded waveform is shown in **Figure 6.** The signal exhibited continuous pulsatile morphology, stable periodicity, and consistent beat-to-beat amplitude. These characteristics are consistent with the expected features of invasive arterial pressure waveforms and indicate that the proposed module was capable of stable waveform acquisition in a clinical setting.

5 Conclusion

This study investigated a high-precision invasive hemodynamic acquisition module based on the AD7124 for multi-channel blood pressure monitoring. The results showed that the proposed system achieved high static measurement accuracy, preliminary low-frequency dynamic waveform reconstruction capability, and stable multi-channel acquisition performance through integrated front-end conditioning, low-noise amplification, precision analog-to-digital conversion, and embedded timing control. These findings indicate that the module can provide high-resolution raw waveform data for subsequent hemodynamic signal analysis and intelligent monitoring applications. The main contribution of this work lies in the development and validation of a compact and scalable hardware–software co-designed acquisition platform that combines measurement precision, electrical safety, and engineering feasibility. Nevertheless, the present study remains limited to bench-top verification and preliminary clinical waveform acquisition, and further evaluation under broader clinical conditions is still required. It should be noted that the present dynamic test was intended as an initial bench-top verification under a representative low-frequency input. A more comprehensive characterization using quantitative indices such as SNR, harmonic distortion, amplitude error, and phase delay across a wider frequency range will be carried out in future work. Future work will focus on improving portability through low-power and wireless design, while introducing adaptive filtering and signal-quality assessment methods to enhance robustness in complex clinical environments.

References

1. B. Saugel, W. Buhre, M.S. Chew, B. Cholley, M. Coburn, B. Cohen, *et al.*, Intra-operative haemodynamic monitoring and management of adults having noncardiac surgery: A statement from the European Society of Anaesthesiology and Intensive Care, Eur. J. Anaesthesiol. **42**, 543–556 (2025).
2. X. Monnet, A. Messina, M. Greco, J. Bakker, N. Aissaoui, M. Cecconi, *et al.*, ESICM guidelines on circulatory shock and hemodynamic monitoring 2025, Intensive Care Med. **51**, 1971–2012 (2025).
3. C. Gaik, P. Paal, D.A. Reuter, H. Wulf, B. Vojnar, Current practices in hemodynamic monitoring and management during non-cardiac surgery in Austria, BMC Anesthesiol. **25**, Article 450 (2025).
4. M. Bertrand, A. Goury, D. Chemla, J.-L. Teboul, O. Hamzaoui, Applied physiology at the bedside: using invasive blood pressure as a true monitoring tool, Ann. Intensive Care **15**, Article 192 (2025).

5. R.C. de Freitas Chaves, C.S.V. Barbas, V.N.F. Queiroz, A. Serpa Neto, R.O. Deliberato, A.J. Pereira, *et al*., Assessment of fluid responsiveness using pulse pressure variation, stroke volume variation, plethysmographic variability index, central venous pressure, and inferior vena cava variation in patients undergoing mechanical ventilation: a systematic review and meta-analysis, Crit. Care **28**, Article 289 (2024).
6. A. Messina, M. Caporale, L. Calabrò, G. Lionetti, D. Bono, G.M. Matronola, *et al*., Reliability of pulse pressure and stroke volume variation in assessing fluid responsiveness in the operating room: a metanalysis and a metaregression, Crit. Care **27**, Article 431 (2023).
7. B. Henry, M. Merz, H. Hoang, G. Abdulkarim, J. Wosik, P. Schoettker, Cuffless Blood Pressure in clinical practice: challenges, opportunities and current limits, Blood Press. **33**, Article 2304190 (2024).
8. S. Kumar, S. Yadav, A. Kumar, Blood pressure measurement techniques, standards, technologies, and the latest futuristic wearable cuff-less know-how, Sens. Diagn. **3**, 181–202 (2024).
9. B.L. Hill, N. Rakocz, Á. Rudas, J.N. Chiang, S. Wang, I. Hofer, *et al*., Imputation of the continuous arterial line blood pressure waveform from non-invasive measurements using deep learning, Sci. Rep. **11**, Article 15755 (2021).
10. *IEC 60601-1: Medical electrical equipment—Part 1: General requirements for basic safety and essential performance*, Edition 3.2, International Electrotechnical Commission (2020).